Cronfa - Swansea University Open Access Repository

_____

This is an author produced version of a paper published in:
The Journal of Engineering

_____

Cronfa URL for this paper:

http://cronfa.swan.ac.uk/Record/cronfa45066

_____

_____

http://www.swansea.ac.uk/library/researchsupport/ris-support/

A New Control Strategy for Low-Voltage Ride-Through of Three-Phase Grid-Connected PV Systems

Hao Wen*, Meghdad Fazeli†

*College of Engineering, Swansea University, Bay Campus, Swansea, Wales, United Kingdom, 688418@swansea.ac.uk

† College of Engineering, Swansea University, Bay Campus, Swansea, Wales, United Kingdom, M.Fazeli@swansea.ac.uk

Abstract

Power quality and current limitation are the most important aspects of the grid-connected power converters under fault. Since the distributed energy resources are widely used, fault management strategy is important for micro-grids applications. This paper presents a new control strategy for low-voltage ride-through for 3-phase grid-connected photovoltaic systems. The proposed method, which is designed in synchronous frame using positive and negative sequence components, can protect the inverter from overcurrent failure under both symmetrical and unsymmetrical faults and provides reactive power support. The method does not require a hard switch to switch from MPPT to a non-MPPT algorithm, which ensures a smooth transition.

1 INTRODUCTION

During the last decades, the use of distributed energy resources (DERs) has increased due to economical, technical and environment concerns [1], [2]. Micro-grids (MGs) have emerged as a potential solution for integrating DERs into the distribution networks operating in grid-connected mode [3]. Photovoltaic (PV) generation as the commonly used DERs should contribute to the grid stability by providing high quality services, beyond the basic power delivery [4]- [7]. According to the recently revised grid codes, PV systems are supposed to stay in grid-connected mode during faults [8]. When a fault occurs, the converter should have a quick response to the disturbance to eliminate the effect on the inverter and the grid. Furthermore, a certain amount of reactive power need to be injected to support the grid when a low voltage fault is occurred [9]. This capability is known as low voltage ride-through (LVRT).

Different methods have been presented in the literature. For example, in [3], a control strategy for limiting the inverter current based on an islanded system is presented. However, the LVRT strategy in grid-connected PV is a big challenge. From simulation test, the dynamics of the PV array (including

Maximum Power Point Tracking (MPPT) algorithm), the capacitive dc-link voltage control and the current loop controller can affect the operation of the entire system. Moreover, in [3], the current is limited to 2 pu during both symmetrical and unsymmetrical fault, which seems to be too high for slightly voltage sag of unsymmetrical faults. In [8], where the operation of a two-stage 3-phase grid-connected PV system is discussed, a fault detecting algorithm is needed to switch from MPPT mode to a non-MPPT mode. In addition, this paper only discusses the behavior of their strategy for unsymmetrical fault. In [10], an instantaneous active power controller is presented, which results to non-sinusoidal inverter current under unbalanced fault. Reference [11] has proposed an LVRT control scheme using the symmetrical components in synchronous frame for grid-connected inverter without considering the renewable energy sources, neither a PV nor a wind turbine. This is important as a comprehensive method must take the input power from the intermittent source into account such that it limits the input power during faults without disturbing MPPT during normal operation.

In light of the above, the proposed LVRT scheme in this paper is able to:
1) Operate for both symmetrical and unsymmetrical faults.
2) Limit the current to 2 pu during 3-phase fault without activating the inverter overcurrent protection.
3) Limit the current to 1.5 pu during unbalanced faults.
4) Provide high quality sinusoidal voltage and current during all types of faults.
5) Eliminate the need to switch from MPPT mode to non-MPPT mode.

The paper is structured as follow: In Section II, the proposed LVRT control scheme is presented, including the method to estimate the positive sequence and negative sequence components for voltage and current in synchronous frame, voltage loop design with the proposed current limiting strategy, reactive power injection and current loop design. The proposed control strategy is verified by MATLAB/Simulink simulations in Section III. Finally, conclusions are drowned at the end to summarize the advantage of the proposed method in Section IV.
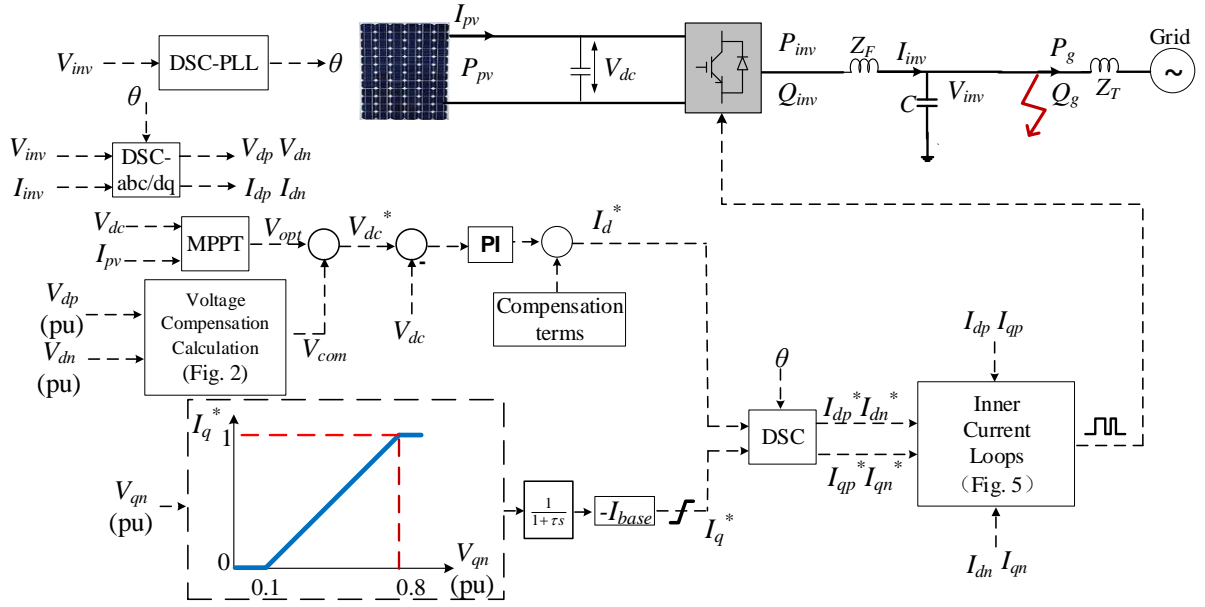
Figure 1: The system understudy plus the proposed control scheme for grid-connected PV.
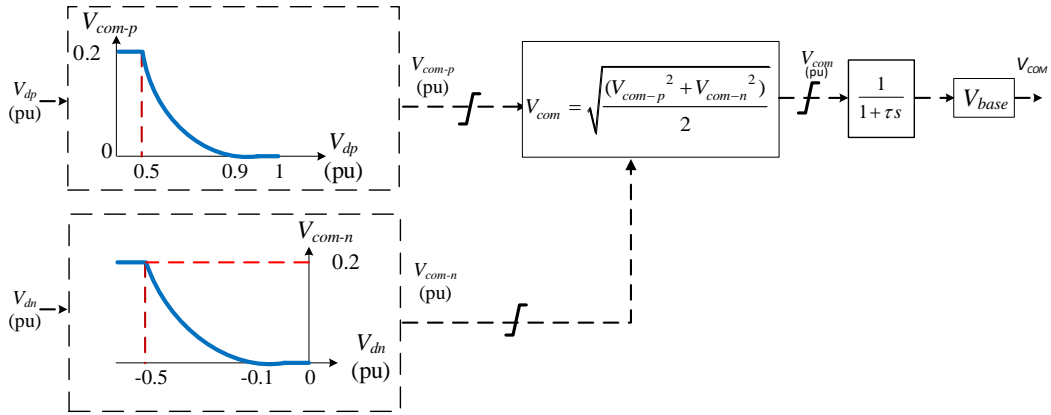

Figure 2: Structure of the proposed voltage compensation calculation unit.

2 PROPOSED CONTROL STRATEGY

The system understudy plus the proposed LVRT strategy are illustrated in Fig.1. The proposed control strategy uses the classic cascaded voltage and current loops in dq-frame, which includes a proposed Voltage Compensation Calculation (VCC) unit (detailed in Fig. 2). The current loop consists of four PI controllers for dq-currents in positive (I_{dp}, I_{qp}) and negative (I_{dn}, I_{qn}) sequences (see Fig.5). The Delayed Signal Cancellation (DSC) method, explained in [12], is used to get the symmetrical components of the inverter voltage V_{inv} and inverter current I_{inv}, while a DSC-PLL, which introduced in [13] synchronizes the system with the grid. A reactive power injection block is proposed, which determined how much reactive power should be injected during fault. The proposed scheme is detailed below:

2.1 Symmetrical Components Generation

In this paper, the well-known method of DSC is used for sequence component separation. The DSC method, which is detailed in [12], uses:

$$V_{p(\alpha,\beta)} = \frac{1}{2}\left[V_{\alpha,\beta}(t) + jV_{\alpha,\beta}\left(t - \frac{T}{4}\right)\right] \qquad (1)$$

$$V_{n(\alpha,\beta)} = \frac{1}{2}\left[V_{\alpha,\beta}(t) - jV_{\alpha,\beta}\left(t - \frac{T}{4}\right)\right] \qquad (2)$$

In Equations (1) and (2), $V_{p(\alpha,\beta)}$, $V_{n(\alpha,\beta)}$ are the estimations of the positive and negative sequence signals in stationary frame; T is the signal period, which is the same as the grid period. The symmetrical components for current can be estimated using (1) and (2) as well. Then both voltage and current signals are converted to synchronous frame using the standard Park Transform.

2.2 Voltage Loop with Voltage Compensation Calculation

Since the control strategy aims to limit the inverter current during balanced and unbalanced faults while the PV array is still running without disabling the MPPT, the proposed VCC unit is applied. As it is shown in Fig. 2, the proposed VCC unit determines the reference DC-link voltage V_{dc}^* through adding a compensation value V_{com} to the optimum value V_{opt}, provided by

the MPPT algorithm. The amended DC-link reference voltage V_{dc}^* determines the reference d-component current I_d^* through a standard voltage loop using a PI controller. The VCC is designed to force the PV array to produce less power during fault compare to the steady state operation. As it can be seen from P_{pv}-V_{pv} characteristic in Fig. 3, it is possible to reduce P_{pv} through either adding V_{com} to V_{opt} or subtracting V_{com} from V_{opt}. However, considering the I_{pv}-V_{pv} curve, it can be easily found that only when the PV is operating at the right side of the MPP (Shadowed Area), the output current of the PV can be reduced i.e. when V_{com} is added to V_{opt}:

$$V_{dc}^* = V_{opt} + V_{com} \tag{3}$$

For example, through using Equation (3), therefore, when a fault occurs, the system will be operating at the fault operation point (FOP) shown in Fig. 3, where both P_{pv} and I_{pv} are reduced, leading to a reduced inverter current. In addition, the system is stable when the operation point is located at the right side of the MPP [14].
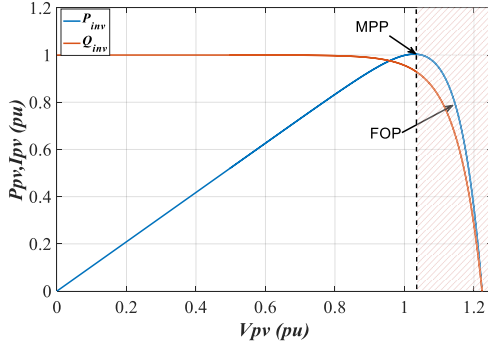

Figure 3: P_{pv}-V_{pv} & I_{pv}-V_{pv} characteristic curves

The VCC should be designed based on the following principles:

1) The VCC should force the PV system to reduce its active power generated during faults without interrupting MPPT during normal operation.

2) The VCC should be able to obtain the operation point located at the right side of the MPP.

3) The VCC should have a quick response when the voltage sag is sever and a slow response when the voltage drop is slightly. This is because if the VCC has a quick response to a slow and small disturbance, the active power of the inverter will become unstable. This is achieved through introducing the quadratic functions illustrated in Fig. 2.

As shown in Fig. 2, both positive and negative sequences of V_{inv} d-component (V_{dp}, V_{dn}) are used in this proposed method. V_{com} is calculated by both V_{com-p} and V_{com-n}, where V_{com-p} and V_{com-n} are generated by V_{dp} and V_{dn} variations, respectively: V_{dp} is 1pu during normal operation and reduces after both symmetrical and unsymmetrical faults. Considering 10% tolerant, V_{com-p} can be calculated as Equation (4):

$$V_{com-p} = -\Delta V_{dp}\left(V_{dp} - 0.9\right) \tag{4}$$

Where ΔV_{dp} is the voltage sag of V_{dp}. Using Equation (4), which is simply the quadratic curve shown in Fig. 2, leads to a

higher rate of increase in V_{com-p} as ΔV_{dp} increases. On the other hand, V_{dn}, which is zero during normal operation, decreases following only unsymmetrical faults. Considering 10% tolerant, V_{com-n} can be calculated as Equation (5):

$$V_{com-n} = \Delta V_{dn}\left(-V_{dn} - 0.1\right) \tag{5}$$

Where ΔV_{dn} is the voltage sag of V_{dn}. Using Equation (5) leads to a higher rate of increase in V_{com-n} as ΔV_{dn} increases. Note that V_{dn} is negative and ΔV_{dn} is positive. Both V_{com-p} and V_{com-n} are limited to V_{oc} - $V_{opt-max}$, where V_{oc} is the PV array open circuit voltage and $V_{opt-max}$ is the V_{opt} at 1 pu solar power. By doing this, it is ensured that V_{dc}^* remains smaller than V_{oc}. Since in the simulated model V_{oc} - $V_{opt-max}$ =0.2 pu, 0.2 pu is used in Fig. 2. Thus, from Equations (4) and (5), when both V_{dp} and V_{dn} sags depth under 0.5 pu, V_{com-p} and V_{com-n} will reach the limitation (0.2 pu). V_{com} will be calculated through using Root-Mean-Square Deviation (RMSD) of the positive and negative sequence compensation terms V_{com-p} and V_{com-n}, in order to ensure that V_{com} remains under 0.2 pu as well. A Low-Pass-Filter (LPF) is used to add dynamics to the system, which reduces the oscillations at the fault occurring and clearing instances. A classic PI controller is used for the voltage loop to get I_d^*, which is the reference d-component current.
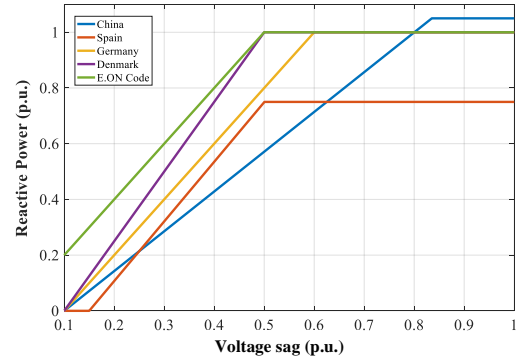
2.3 Reactive Power Injection

Figure 4: Grid Standards of each country.

Considering the grid standard of each country present in [8], Fig. 4 depicts how much reactive power must be injected in respect to the voltage sag in different countries. According to [15], a PV plant must be equipped with reactive power control function capable of controlling the reactive power supplied by the PV power plant. Since the DSC-PLL keeps the positive sequence of V_{inv} q-component $V_{qp} \approx 0$ (at steady state), the negative sequence V_{qn} is proposed for reactive power regulation. V_{qn}=0 during normal operation, thus, as V_{qn} increases after a fault, the reference I_q^* increases. This paper uses the Chinese standard such that for V_{qn}<0.1 pu; I_q^*=0, for V_{qn}>0.8 pu, I_q^*=1.05 pu, and 0.1<V_{qn}<0.8 pu, I_q^* varies linearly.

2.4 Current Loop

As illustrated in Fig. 5, the current loop consists of four classic PI controllers for positive and negative sequences of d- and q-components. The modulating signal m is calculated through adding the positive and negative modulating signals $m=m_p+m_n$, while m_p and m_n are calculated through using the inverse Park

transform. It is noted that the phase angle used in the negative channel is $-\theta$.
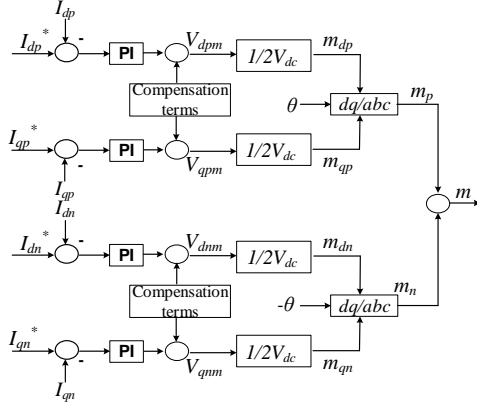

Figure 5: Current Loop.

The integral gain of the PI controllers is designed using the characteristic equation:

$$s^2 + (\frac{R_f + K_p}{L_f})s + \frac{K_i}{L_f} = 0 \tag{6}$$

In Equation (6), R_f and L_f are the LC filter impedance. Choosing the bandwidth to be ω_n= 1759 rad/s (f_n=280 Hz), the integral gain $K_i=L_f\omega_n^2= 9234.67$. Considering the PI controller should be robust enough when fault occurs, from Equation (6) the proportional gain K_p can be designed as follow:

$$s^2 + \frac{R_f}{L_f}s + \frac{K_i}{L_f} + \frac{K_p}{L_f}s = 0$$

$$s^2 + \frac{R_f}{L_f}s + \frac{K_i}{L_f} = -\frac{K_p}{L_f}s$$

$$1 = \frac{-\dfrac{K_p}{L_f}s}{s^2 + \dfrac{R_f}{L_f}s + \dfrac{K_i}{L_f}}$$

$$1 + \frac{\dfrac{K_p}{L_f}s}{s^2 + \dfrac{R_f}{L_f}s + \dfrac{K_i}{L_f}} = 0 \tag{7}$$

Equation (7) is basically the characteristic equation, thus, from the definition of characteristic equation, the equivalent Open Loop Transfer Function (OLTF) for this proposed control plant, which contains the open loop gain K_p (It is the proportional gain of the current loop) can be written as Equation (8):

$$OPLF = \frac{\dfrac{K_p}{L_f}s}{s^2 + \dfrac{R_f}{L_f}s + \dfrac{K_i}{L_f}} \tag{8}$$

Where, K_i is calculated above. The Root locus chart can be drawn based on K_p. Fig. 6 is the Root locus diagram of this proposed current loop. Normally K_p is chosen smaller than 9.83, which is the critically damping point (ξ=1). However, here K_p=82.5, where $\xi >1$ is used to enhance the system robustness during fault. Note that this high proportional gain will not affect the system's stability, which can be seen from Fig. 6. Also, the operation of the system when irradiation is varied will not be affected by this K_p.
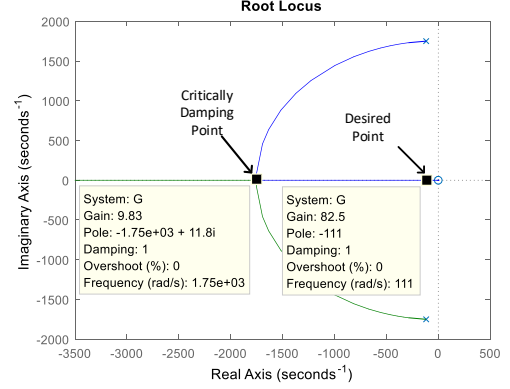

Figure 6: Root locus diagram of the proposed current loop.

3 SIMULATION RESULTS AND ANALYSIS

In this section, the proposed control strategy is simulated in MATLAB/SIMULINK environment. The frequency of the grid is f = 50Hz. The rest of the parameters are shown in Table 1. Note that all results are presented in pu based on P_{rating}=1 pu.

Variable	Value
Line to Line voltage V_{L-L}	650 V
DC link capacitor C_{dc}	800 μF
LC filter parameters	R_f=0.7 Ω L_f =3 mH
Line Impedance	R_l = 0.38 Ω L_l =0.15 mH
VCC's LPF time constant (τ)	0.06 s

Table 1: System Parameters

Both symmetrical and unsymmetrical faults are simulated. For all the simulation, the fault occurs at t=1 s and lasts for 0.2 s.
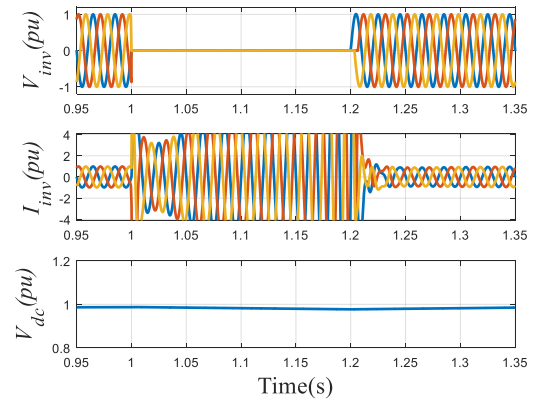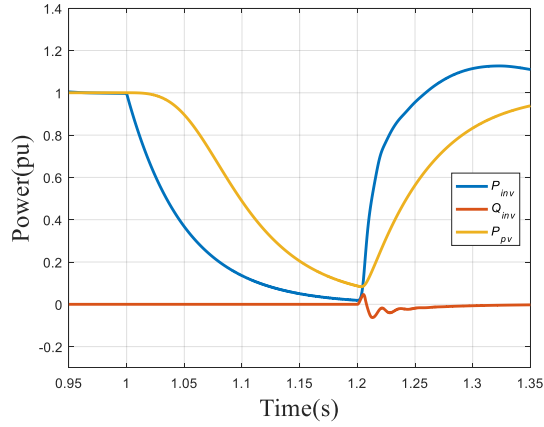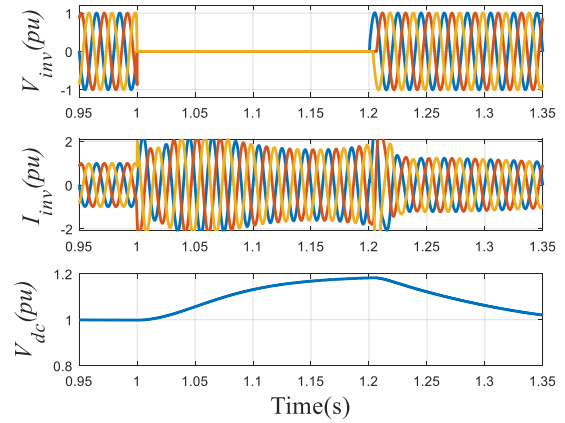
3.1 Results under 3-phase to ground fault

Figure 7: Simulation results of the PV system during a 3-phase to ground fault without LVRT. 3-phase Inverter Voltage, Current and DC-link Voltage.

4

(a)   (b)

Figure 8: Simulation results of the PV system during a 3-phase to ground fault with LVRT. (a) Active and reactive power of the inverter and PV array power, (b) 3-phase Inverter Voltage, Current and DC-link Voltage.
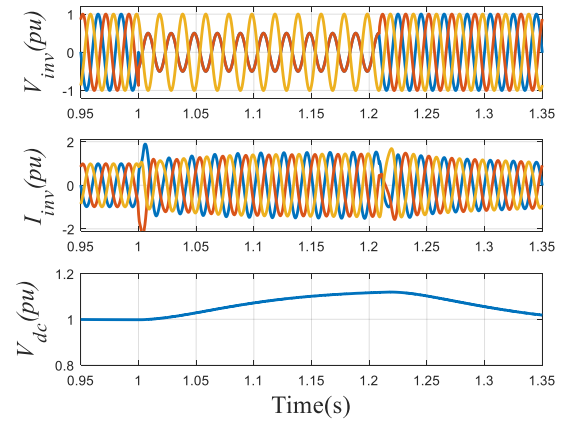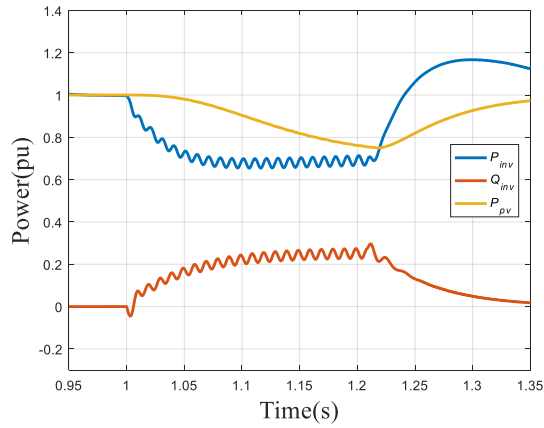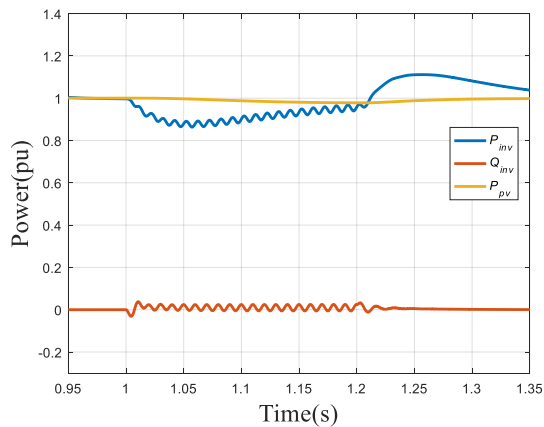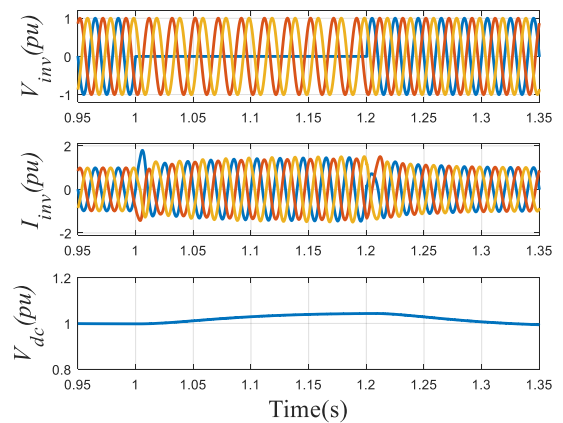

Figure 9: Simulation results of the PV system during a double line fault with LVRT. (a) Active and reactive power of the inverter and PV array power, (b) 3-phase Inverter Voltage, Current and DC-link Voltage.

(a)   (b)

Figure 10: Simulation results of the PV system during a line to ground fault with LVRT. (a) Active and reactive power of the inverter and PV array power, (b) 3-phase Inverter Voltage, Current and DC-link Voltage.

Figure 7 shows both the 3-phase voltage V_{inv} and current I_{inv} and the DC-link voltage with the conventional control strategy i.e. no LVRT strategy. As it can be seen, once the fault occurs, the 3-phase voltage V_{inv} falls to almost zero, and 3-phase current I_{inv} increases dramatically (I_{inv} is much higher than the 2 pu hard limit during the whole fault period, which will result

to an overcurrent failure for the inverter). However, as shown in Fig. 8 with the proposed controller, the 3-phase currents I_{inv} hit the hard limit for only less than 0.02second. Then it is reduced to less than 2pu. Note that the inverter protection system will not be activated during such a short period of time. The power generated by the PV array is reduced after fault, thus, the active power of the inverter is reduced. After the fault is cleared, the PV system will restore its normal operation.

3.2 Results under Double Line (DL) fault

Figure 9 shows the simulation results for a double line fault using the proposed method. As it can be seen, the proposed method reduces P_{pv} through increasing V_{dc}, which results to I_{inv} limited to less than 1.5 pu. Since the voltage on the healthy phase remains at 1 pu and both I_{inv} and V_{inv} remain sinusoidal during the fault, it is possible to keep feeding the loads connected to the healthy phase. The normal operation is restored as soon as the fault is being cleared.

3.3 Results under Single Line to Ground (LG) fault

Figure 10 shows the simulation results for a single line to ground fault using the proposed strategy. Since the voltage on the two healthy phases remain at 1pu during fault, the 3-phase voltage drop is slightly less than 3-phase fault and DL fault. Therefore, V_{com}, which is calculated by the VCC is smaller than the other types of fault, leading to P_{pv} falls not significantly (almost remain at 1 pu). Meanwhile, I_{inv} is limited to less than 1.5pu without hitting the hard limit.

4 CONCLUSION

This paper proposes a LVRT control strategy for grid-connected PV systems. The method is based on the classic cascaded voltage and current loops in dq-frame, while the positive and negative sequences of d-component voltage is used to adjust the reference DC-link voltage to limit the inverter current during a voltage sag. The q-component current is used to supply the required reactive power to restore the voltage. The proposed method is validated in MATLAB/SIMULINK. Simulation results show that the proposed LVRT control strategy can be used for both balanced and unbalanced faults. The presented results show that the for a sever voltage sag (3-phase fault), the propose method could significantly reduce the fault current to protect the inverter from overcurrent failure. For a lighter voltage sag, for instant, the LG fault, which is the most commonly fault, the proposed method could limit the fault current to a reasonable level with little affect to the utility system (supplying the grid/loads with reduced active power since the voltage and current remain sinusoidal during fault.) The method does not require a hard switch to switch from MPPT to a non-MPPT algorithm, which ensures a smooth transition.

REFERENCES

[1] Olivares, D.E., Mehrizi-Sani, A., Etemadi, A.H., Cañizares, C.A., Iravani, R., Kazerani, M., Hajimiragha, A.H., Gomis-Bellmunt, O., Saeedifard, M., Palma-Behnke, R., Jiménez-Estévez, G.A., and Hatziargyriou, N.D.: 'Trends in Microgrid Control', *IEEE Transactions on Smart Grid*, **vol. 5**, no. 4, pp. 1905-1919, (2014).

[2] B. Lasseter, 'Microgrids,' in Proc. IEEE Power Eng. Soc. Winter Meeting, **vol. 1**. Columbus, OH, USA, pp. 146–149, (2002).

[3] Sadeghkhani, I., Hamedani Golshan, M.E., Guerrero, J.M., and Mehrizi-Sani, A.: 'A Current Limiting Strategy to Improve Fault Ride-Through of Inverter Interfaced Autonomous Microgrids', *IEEE Transactions on Smart Grid*, **vol. 8**, no. 5, pp. 2138-2148, (2017).

[4] R. Meyer, A. Zlotnik, and A. Mertens, 'Fault ride-through control of medium-voltage converters with LCL filter in distributed generation systems,' *IEEE Trans.Ind.* Appl., **vol. 50**, no. 5, pp. 3448–3456, Sep./Oct, (2014).

[5] J. Hu, Y. He, L. Xu, and B. W. Williams, 'Improved control of DFIG systems during network unbalance using PI–R current regulators,' *IEEE Trans. Ind. Electron.*, **vol. 56**, no. 2, pp. 439–451, Feb, (2009).

[6] A. Camacho, M. Castilla, J. Miret, J. C. Vasquez, and E. Alarcon-Gallo, 'Flexible voltage support control for three phase distributed generation inverters under grid fault,' *IEEE Trans. Ind. Electron.*, **vol. 60**, no. 4, pp. 1429–1441, Apr, (2013).

[7] J. Miret, M. Castilla, A. Camacho, L. G. D. Vicu, and J. Matas, 'Control scheme for photovoltaic three-phase inverters to minimize peak currents during unbalanced grid-voltage sags,' *IEEE Trans. Power Electron.*, **vol. 27**, no. 10, pp. 4262–4271, Oct, (2012).

[8] Afshari, E., Moradi, G.R., Rahimi, R., Farhangi, B., Yang, Y.H., Blaabjerg, F., and Farhangi, S.: 'Control Strategy for Three-Phase Grid-Connected PV Inverters Enabling Current Limitation Under Unbalanced Faults', *IEEE Trans. Ind.Electron*, **vol. 64**, no. 11, pp. 8908-8918, (2017).

[9] R. Meyer, A. Zlotnik, and A. Mertens, 'Fault ride-through control of medium-voltage converters with LCL filter in distributed generation systems,' *IEEE Trans. Ind.* Appl., **vol. 50**, no. 5, pp. 3448–3456, Sep./Oct, (2014).

[10] R. Teodorescu, M. Liserre, and P. Rodriguez, 'Grid Converters for Photovoltaic and Wind Power Systems', **vol. 29**. Hoboken, NJ, USA: Wiley, (2011).

[11] S. Alepuz et al., 'Control strategies based on symmetrical components for grid-connected converters under voltage dips,' *IEEE Trans. Ind.Electron.*, **vol. 56**, no. 6, pp. 2162–2173, Jun, (2009).

[12] Cárdenas, R., Dı́az, M., Rojas, F., and Clare, J.: 'Fast Convergence Delayed Signal Cancellation Method for Sequence Component Separation', *IEEE Transactions on Power Delivery*, **vol. 30**, no. 4, pp. 2055-2057, (2015).

[13] Huang, Q., and Rajashekara, K.: 'An Improved Delayed Signal Cancellation PLL for Fast Grid Synchronization Under Distorted and Unbalanced Grid Condition', *IEEE Transactions on Industry Applications*, **vol. 53**, no.5, pp. 4985-4997, (2017).

[14] Egwebe, A.M., Fazeli, M., Igic, P., and Holland, P.M.: 'Implementation and Stability Study of Dynamic Droop in Islanded Microgrids', *IEEE Transactions on Energy Conversion*, **vol. 31**, no. 3, pp. 821-832, (2016).

[15] D. Energinet, 'Technical regulation 3.2.2 for PV power plants with a power output above 11 kW,' Energinet, Fredericia, Denmark, Tech. Rep., (2015).